

Supplementary Information

**Rh(III) catalyzed C–H activation of 4+1 annulation of sulfoxonium ylide with
Allyl Alkyl Ether: Detailed theoretical study of DFT and towards the anti-
inflammatory and antidiabetic activity**

**Pakkirisamy Sivakumar^{a,f}, Pothapragada S. K. Prabhakar Ganesh^b, Perumal Muthuraja^{c,e},
Sarangapani Bharanidharan^d, Balasubramaniyan Anandhan^a, Rajaram Rajamohan^{e*},
Subramaniyan Kamatchi^{f*}**

^a Department of Chemistry, Saraswathy College of Engineering and Technology, Olakkur,
Tindivanam- 604 305, Tamil Nadu, India.

^b Department of Chemistry, Indian Institute of Science Education and Research (IISER) Tirupati,
Tirupati - 517 507, Andhra Pradesh, India.

^c Department of Chemistry, Indian Institute of Technology Guwahati, Guwahati - 781 039, Assam,
India.

^d Department of Physics, Panimalar Engineering College, Chennai - 600 123, Tamil Nadu, India.

^e Organic Materials Synthesis Laboratory, School of Chemical Engineering, Yeungnam
University, Gyeongsan 38541, Republic of Korea.

^f PG & Research Department of Chemistry, Government Arts College, Chidambaram - 608 102,
Tamil Nadu, India.

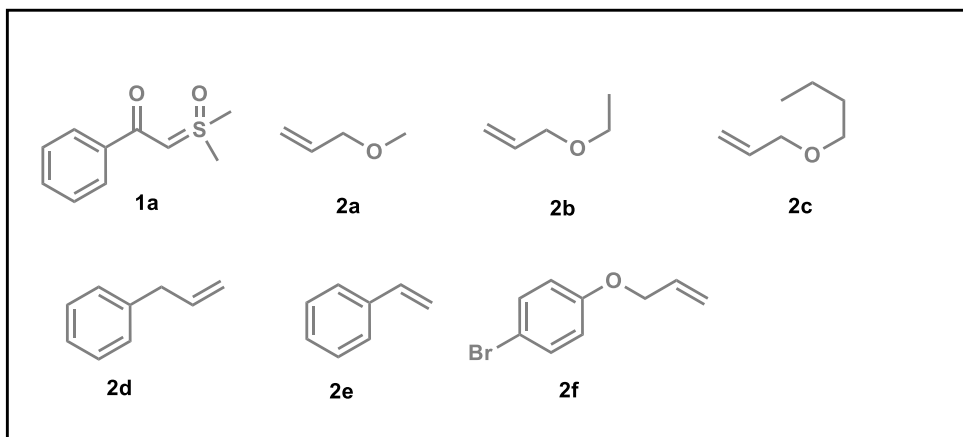
E-mail: rajmohanau@yu.ac.kr (R.R); drskgaccdmchem@gmail.com (S.K)

1.0 General remarks

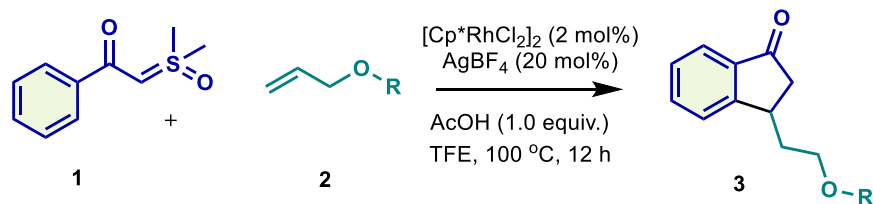
All experiments were carried out in the open air unless stated otherwise. Merck precoated silica gel plates (Art. 5554) treated with a fluorescent indicator were used for analytical thin layer chromatography (TLC). Column chromatography was performed using silica gel 9385 (Merck). Melting points are uncorrected and were determined using the Fisher-Johns Melting Point Apparatus. ^1H NMR (400 MHz), ^{19}F NMR (376 MHz), and ^{13}C NMR (100 MHz) spectra were recorded on the Bruker AVANCE NEO 400 MHz spectrometer. The NMR spectra were recorded in CDCl_3 using $\delta = 7.26$ for ^1H NMR and 77.16 for ^{13}C NMR, ppm as the residual solvent chemical shifts. The NMR spectra were recorded in $\text{DMSO}-d_6$ using $\delta = 2.50$ and 39.520 ppm as the residual solvent chemical shifts. All chemical shifts (δ) are expressed in units of ppm and J values are given in Hz. Multiplicities are abbreviated as follows: s = singlet, d = doublet, t = triplet, q = quartet, m = multiplet or overlap of nonequivalent resonances, and dd = doublet of doublets. Melting points were measured with a Fisher Johns melting point apparatus and uncorrected. Infrared (IR) spectra were recorded on a PerkinElmer Spectrum TwoTM IR spectrometer with frequencies expressed in cm^{-1} , and high-resolution mass spectra (HRMS) were obtained from Orbitrap Elite HybridIon Trap-Orbitrap (Thermofischer scientific, Newington, NH, USA) Mass Spectrometer in electrospray ionization mode (ESI+) and Agilent Bio-QTOF-6545high-resolutionion mass spectrometer in electrospray ionization mode (ESI+).

The synthesized sulfoxonium ylides (**1a**), and corresponding allyl alkyl ether (**2a-2c**), styrene (**2e**), and 1-(allyloxy)-4-bromobenzene (**2f**) are commercially available from the TCI and Sigma Aldrich chemicals.

Table S1. Commercially available allyl alkyl ether and synthesis of sulfoxonium ylide



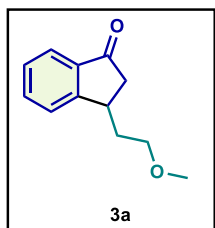
2.0 General procedure for the synthesis of 1,3,4-oxadiazole derivatives (3a)



Phenyl sulfoxonium ylide **1a** (59mg, 0.30 mmol), allyl alkyl ether **2** (0.45 mmol), and $[\text{Cp}^*\text{RhCl}_2]_2$ (3.8 mg, 0.006 mmol), AgBF_4 (11.7 mg, 0.06 mmol) and AcOH (18 mg, 0.3 mmol) dissolved in 2 mL of TFE were combined in a shielded 10 mL vial. This mixture was subjected to a temperature of 100 °C for 12 h. Upon completion, the reaction mixture underwent TLC analysis. Subsequently, the mixture was cooled to room temperature, filtered and the crude was evaporated through rota evaporator and dried under high vacuum. The crude product obtained underwent purification *via* column chromatography, yielding **3a** in 77% (44 mg)

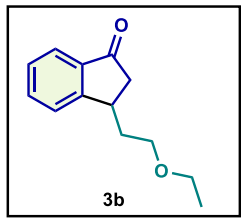
3.0 Characterization data of ^1H , ^{13}C NMR 3a-3c

3-(2-Methoxyethyl)-2,3-dihydro-1H-inden-1-one (3a)



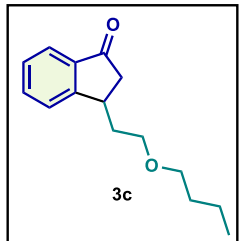
Yield (0.3 mmol scale, 44 mg, 77%); yellow oil; (hexane/ethyl acetate = 8:2, v/v); **FT-IR:** 2875, 1710, 1313, 1256, 953, 723; **^1H NMR** (600 MHz, Chloroform-*d*) δ 7.73 (d, J = 7.8 Hz, 1H), 7.59 (t, J = 7.8 Hz, 1H), 7.50 (d, J = 7.8 Hz, 1H), 7.37 (t, J = 7.8 Hz, 1H), 3.52 – 3.49 (m, 2H), 3.47 – 3.43 (m, 1H), 3.35 (s, 3H), 2.87 (dd, J = 19.2, 7.8 Hz, 1H), 2.42 (dd, J = 19.2, 3.6 Hz, 1H), 2.24 – 2.18 (m, 1H), 1.73 – 1.69 (m, 1H); **^{13}C NMR** (150 MHz, Chloroform-*d*) δ 206.3, 158.5, 136.8, 134.8, 127.7, 125.7, 123.6, 70.9, 58.8, 43.2, 36.0, 35.4; **HR-MS** (ESI) m/z calcd for $\text{C}_{12}\text{H}_{15}\text{O}_2$ [M+H $^+$] 191.1067, found 191.1067.

3-(2-Ethoxymethyl)-2,3-dihydro-1H-inden-1-one (3b)



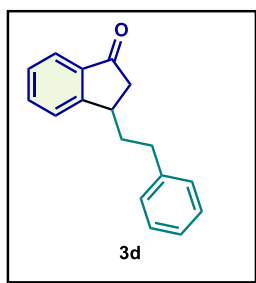
Yield (0.3 mmol scale, 43 mg, 70%); yellow oil; (hexane/ethyl acetate = 8:2, v/v); **FT-IR:** 2888, 1703, 1312, 1253, 946, 727; **^1H NMR** (600 MHz, Chloroform-*d*) δ 7.73 (d, J = 7.8 Hz, 1H), 7.60 (td, J = 7.8, 1.2 Hz, 1H), 7.51 (d, J = 7.8 Hz, 1H), 7.37 (t, J = 7.8 Hz, 1H), 3.57 – 3.44 (m, 5H), 2.87 (dd, J = 19.2, 7.8 Hz, 1H), 2.45 (dd, J = 19.2, 3.6 Hz, 1H), 2.25 – 2.19 (m, 1H), 1.76 – 1.70 (m, 1H), 1.20 (t, J = 7.0 Hz, 3H); **^{13}C NMR** (150 MHz, Chloroform-*d*) δ 206.4, 158.6, 136.8, 134.7, 127.6, 125.8, 123.6, 68.7, 66.5, 43.3, 36.1, 35.6, 15.3; **HR-MS** (ESI) m/z calcd for $\text{C}_{13}\text{H}_{17}\text{O}_2$ [M+H $^+$] 205.1223, found 205.1223

3-(2-Butoxyethyl)-2,3-dihydro-1H-inden-1-one (3c)



Yield (0.3 mmol scale, 58 mg, 73%); yellow oil; (hexane/ethyl acetate = 8:2, v/v); **FT-IR:** 2888, 1703, 1312, 1253, 946, 727; **^1H NMR** (500 MHz, CDCl₃) δ 7.25 (d, J = 8.0 Hz, 1H), 7.13 (t, J = 7.7 Hz, 1H), 7.04 (d, J = 7.5 Hz, 1H), 6.90 (d, J = 7.5 Hz, 1H), 3.76 – 3.50 (m, 1H), 3.10 – 2.89 (m, 3H), 2.65 – 2.37 (m, 3H), 2.01 – 1.93 (m, 1H), 1.80 – 1.66 (m, 1H), 1.17 – 1.04 (m, 2H), 0.95 – 0.85 (m, 2H), 0.44 (td, J = 7.3, 1.5 Hz, 3H); **^{13}C NMR** (126 MHz, CDCl₃) δ 207.0, 159.0, 137.0, 135.1, 127.9, 126.0, 124.0, 71.3, 69.2, 43.5, 36.3, 35.9, 32.1, 19.7, 14.3; **HR-MS** (ESI) m/z calcd for $\text{C}_{15}\text{H}_{21}\text{O}_2$ [M+H $^+$] 233.1536, found 233.1536.

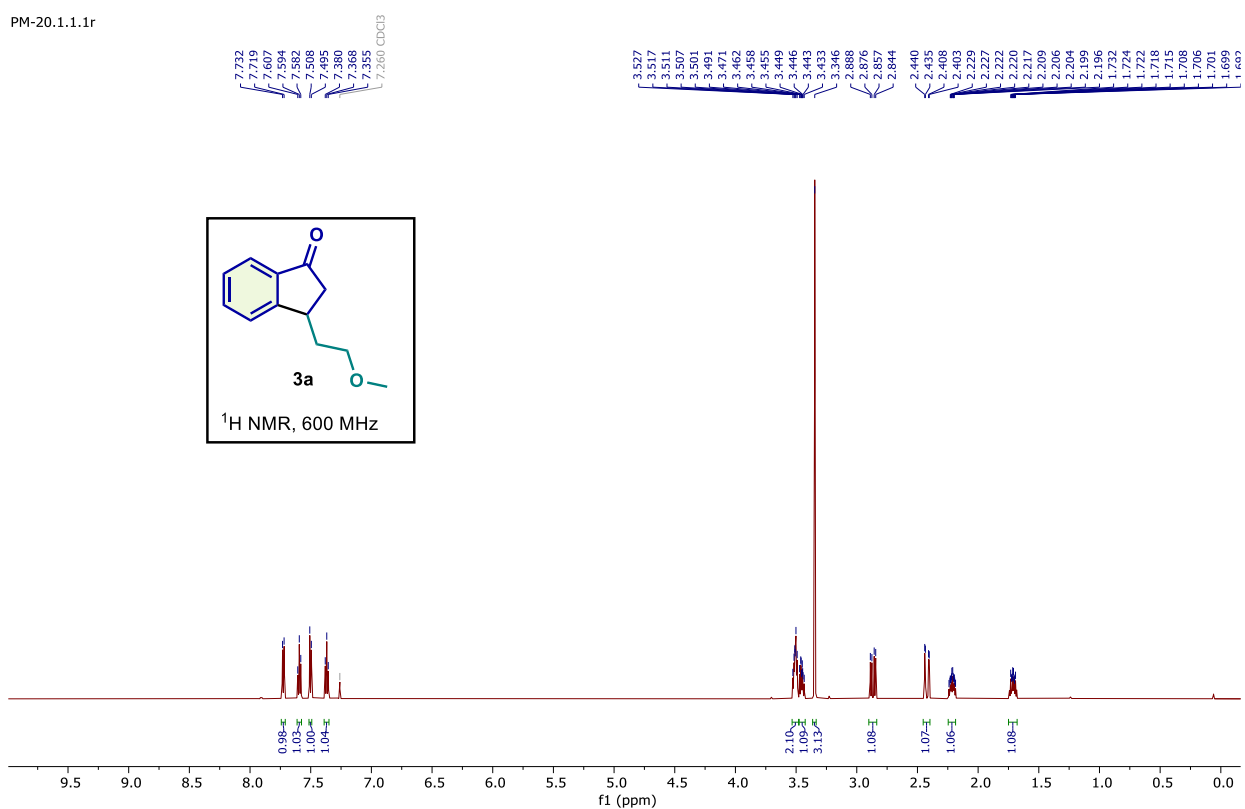
3-Phenethyl-2,3-dihydro-1H-inden-1-one (3d)



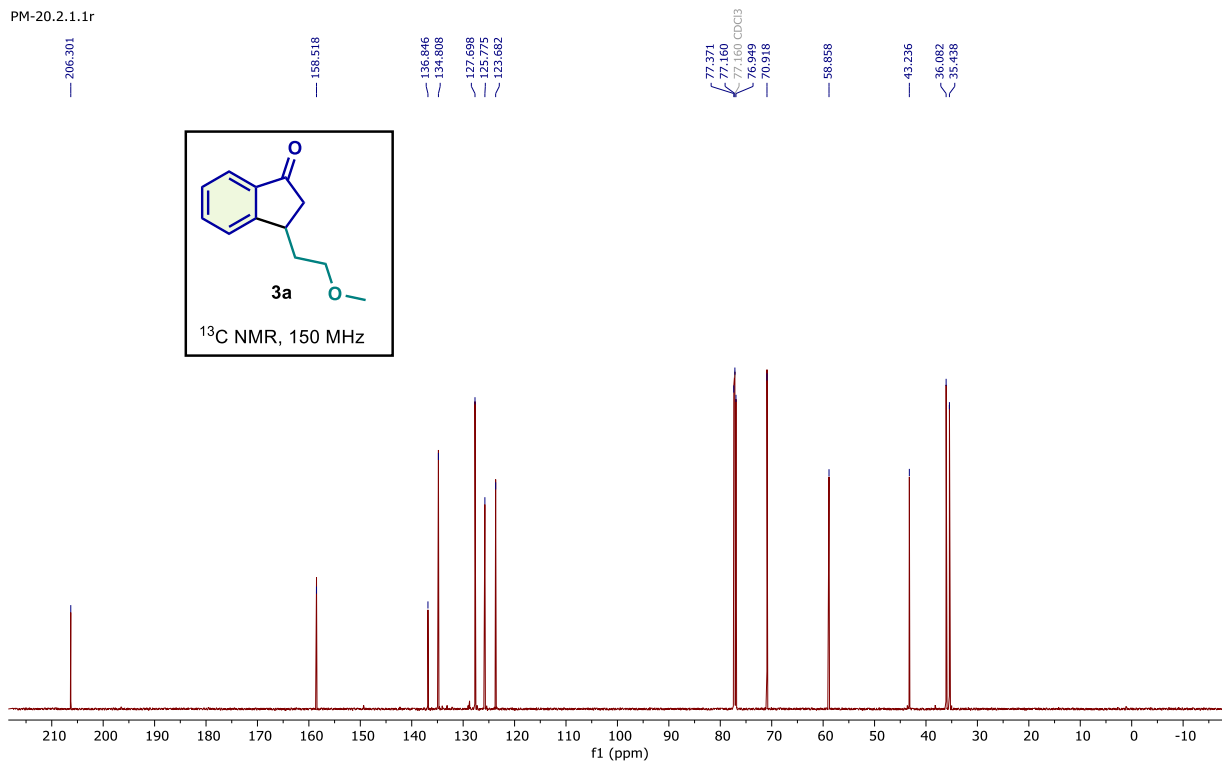
Yield (0.3 mmol scale, 30 mg, 42%); yellow oil; (hexane/ethyl acetate = 8:2, v/v); **¹H NMR** (500 MHz, CDCl₃) δ 7.75 (d, *J* = 7.9 Hz, 1H), 7.60 (t, *J* = 7.6 Hz, 1H), 7.51 (d, *J* = 7.6 Hz, 1H), 7.38 (d, *J* = 14.7 Hz, 2H), 7.31 (d, *J* = 7.6 Hz, 2H), 7.21 (s, 3H), 3.40 (d, *J* = 10.3 Hz, 1H), 2.94 – 2.88 (m, 1H), 2.73 (d, *J* = 5.3 Hz, 2H), 2.44 (d, *J* = 15.5 Hz, 1H), 2.28 (ddt, *J* = 10.2, 6.6, 3.5 Hz, 1H), 1.83 (dd, *J* = 9.4, 4.8 Hz, 1H). **¹³C NMR** (126 MHz, CDCl₃) δ 206.2, 158.6, 141.5, 136.9, 134.8, 128.6, 128.5, 127.7, 126.2, 125.6, 123.7, 43.1, 37.9, 37.9, 34.0. **HR-MS** (ESI) m/z calcd for C₁₇H₁₇O [M+H⁺] 237.1274, found 233.1269.

4.0 Spectrum of ^1H , ^{13}C NMR and HRMS 3a-3d

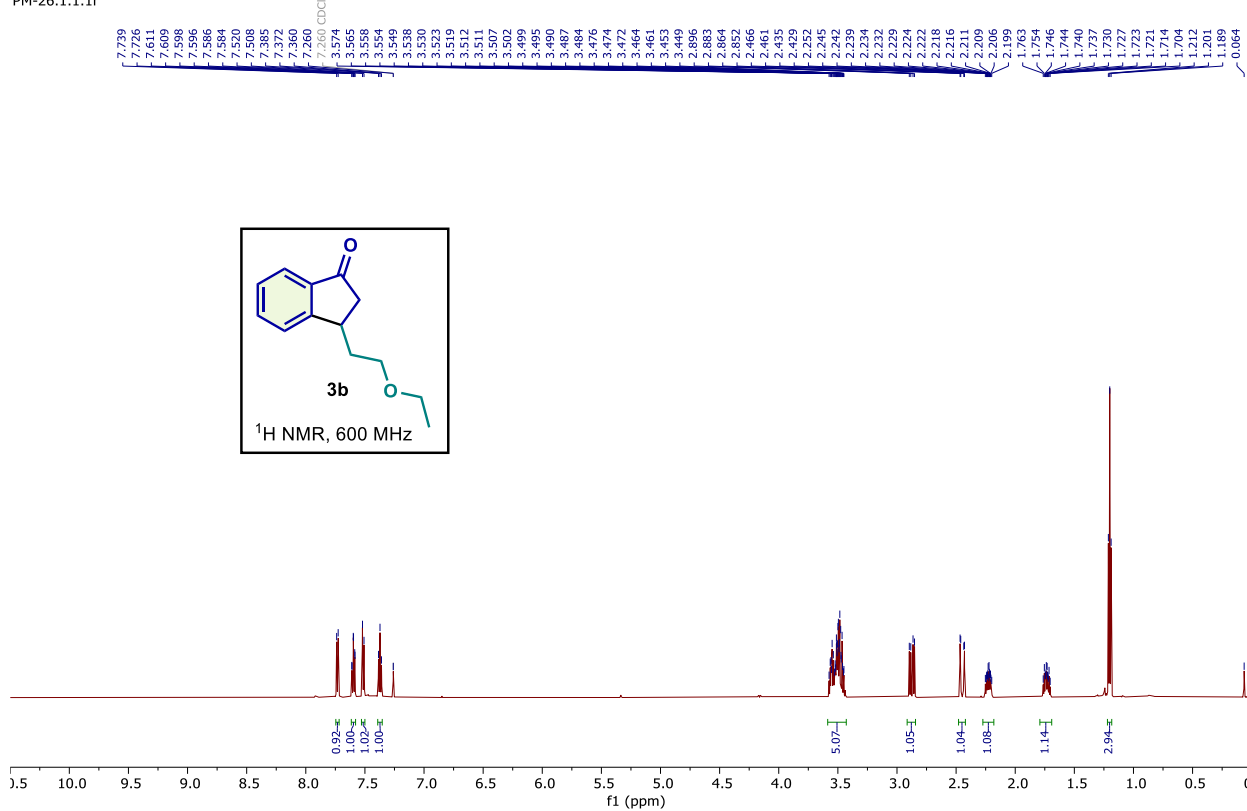
PM-20.1.1.1r



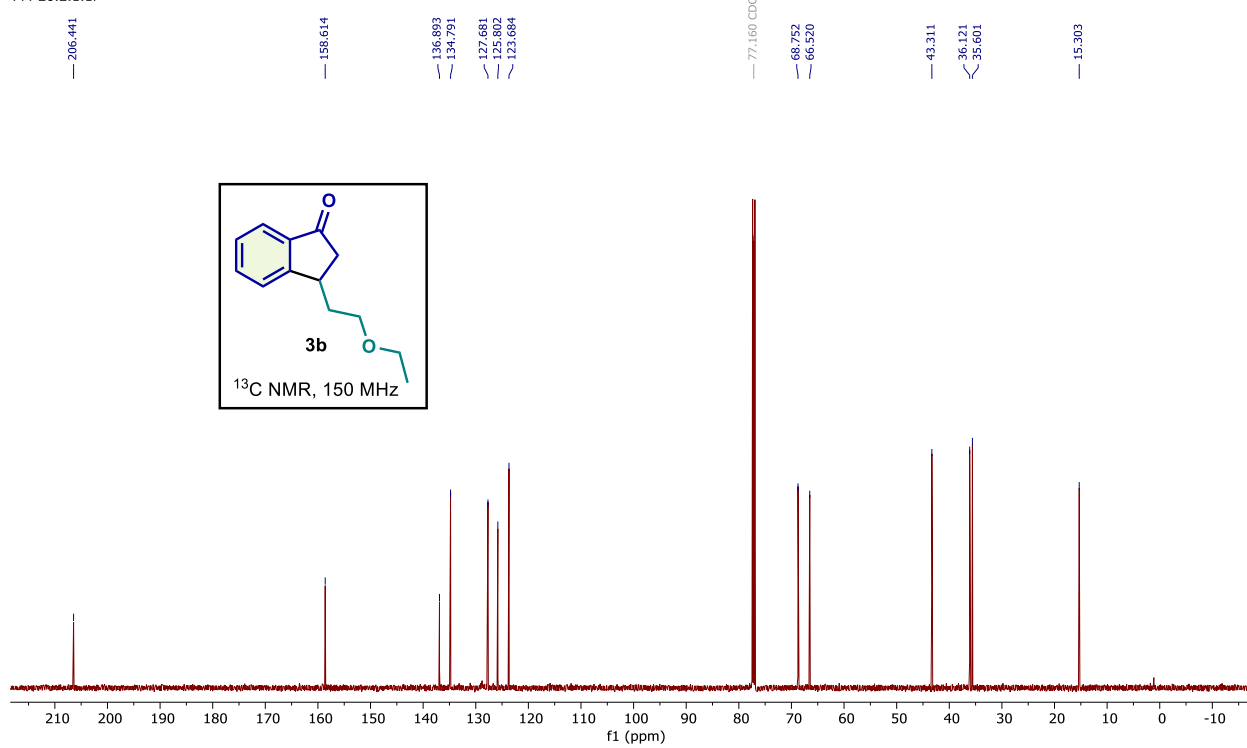
PM-20.2.1.1r



PM-26.1.1.1r



PM-26.2.1.1r



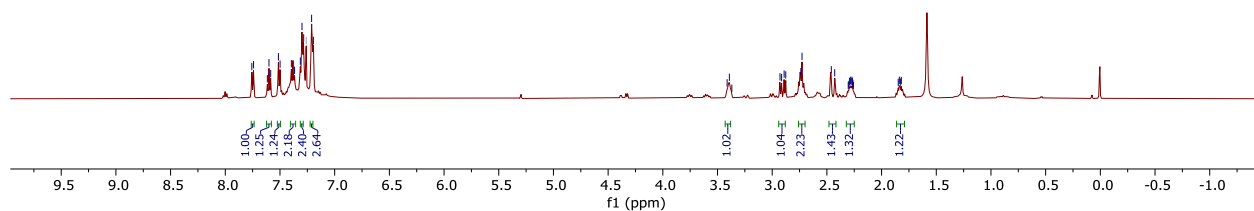
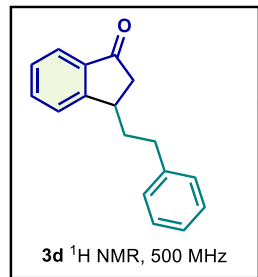
PM-01-BUTYL-1H.5.1.1r
PM-01-BUTYL-1H



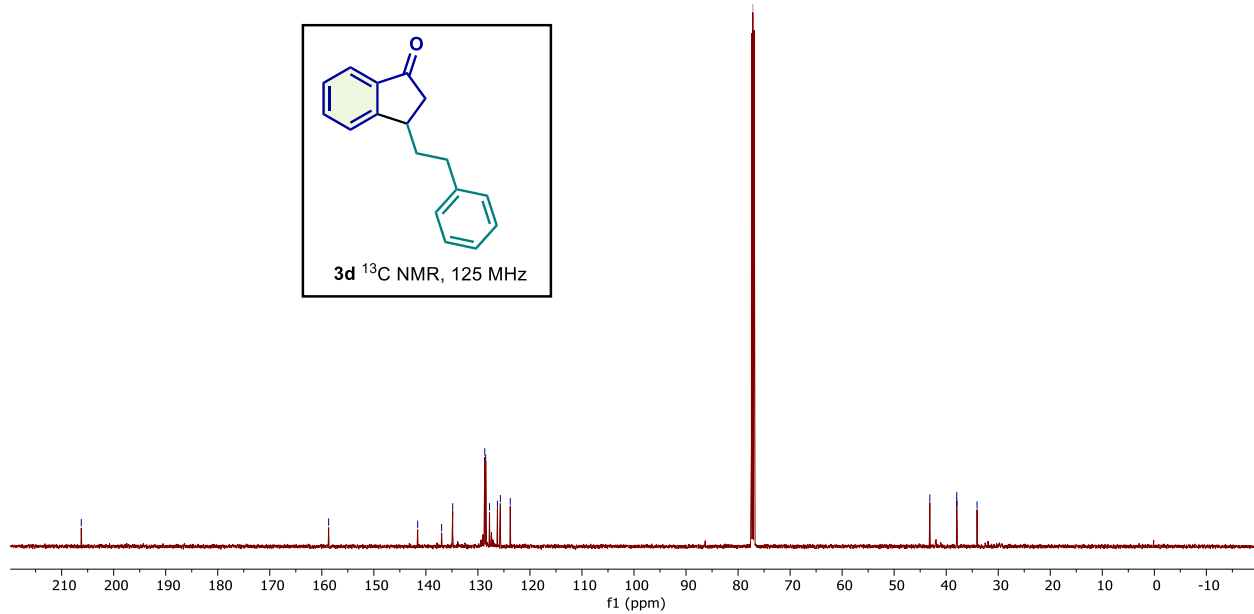
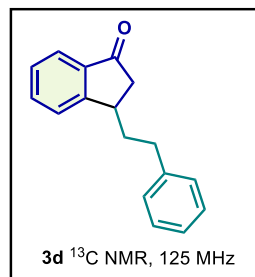
PM-01-BUTYL-13C.7.fid
PM-01-BUTYL-13C



PM-ALLYL-1H.2.1.1r
PM-ALLYL-1H



PM-ALLYL-13C.4.1.1r
PM-ALLYL-13C



Computational details

Using the Gaussian-09W software package^{S1}, theoretical calculations have been carried out using the DFT method with the B3LYP/6-311++G(d,p) basis set. By changing the dihedral angles at the B3LYP/6-311++G(d,p) level of theory, a 3D potential energy scan (PES) was used to look at the most stable conformer of the title molecule. Following geometry optimizations with the DFT method, the HOMO and LUMO energy values as well as the energy gap for compounds (**3a**, **3b**, and **3c**) were calculated using the B3LYP/6-311++G(d,p) basis set. The optimum structures derived from the same level of theory were utilized to illustrate the three-dimensional Molecular Electrostatic Potentials (MEPs) of the compounds featured in the title. Additionally, based on theoretical calculations, the dipole moment, linear polarizability, and first-order hyperpolarizability were determined to demonstrate the nonlinear optical (NLO) activity of the title molecule. Docking calculations were carried out on the DNA Gyrase enzyme protein model.^{S2} Essential hydrogen atoms, Kollman united atom type charges, and solvation parameters were added with the aid of AutoDock tools.^{S3}

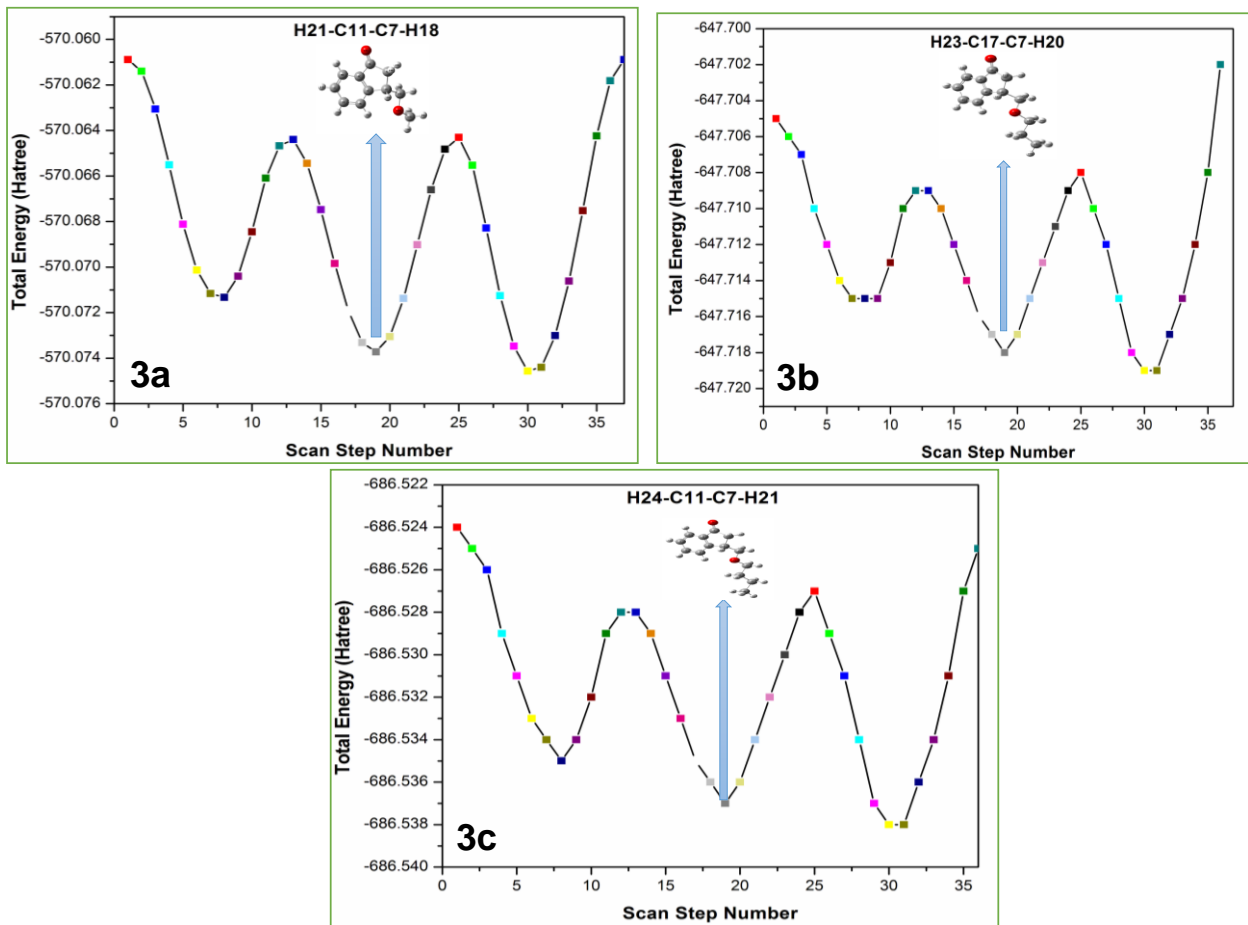


Figure S1. The potential energy surface (PES) scan of compounds 3a, 3b, and 3c.

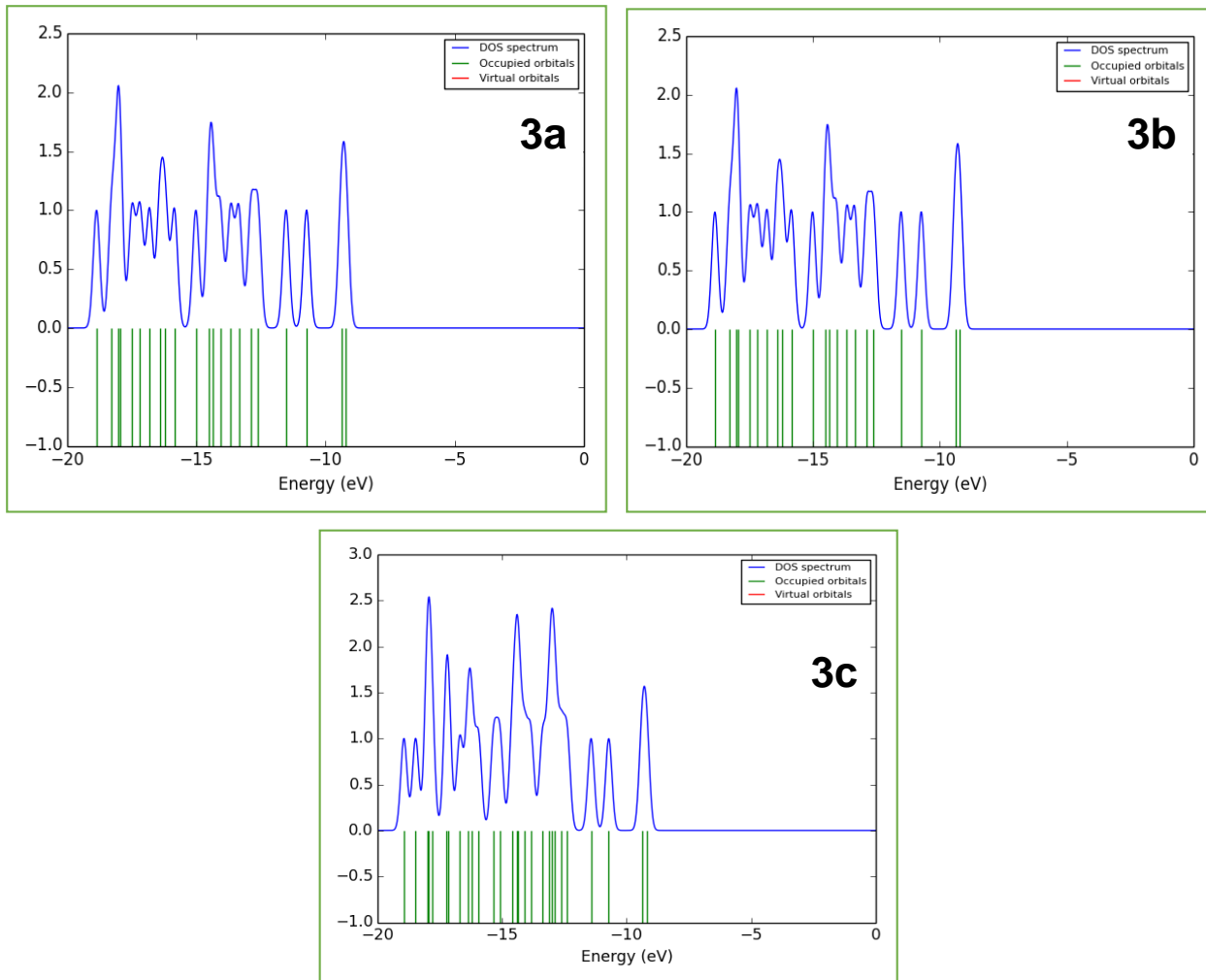


Figure S2. The density of states (DOS) spectra of 3a, 3b, and 3c compounds.

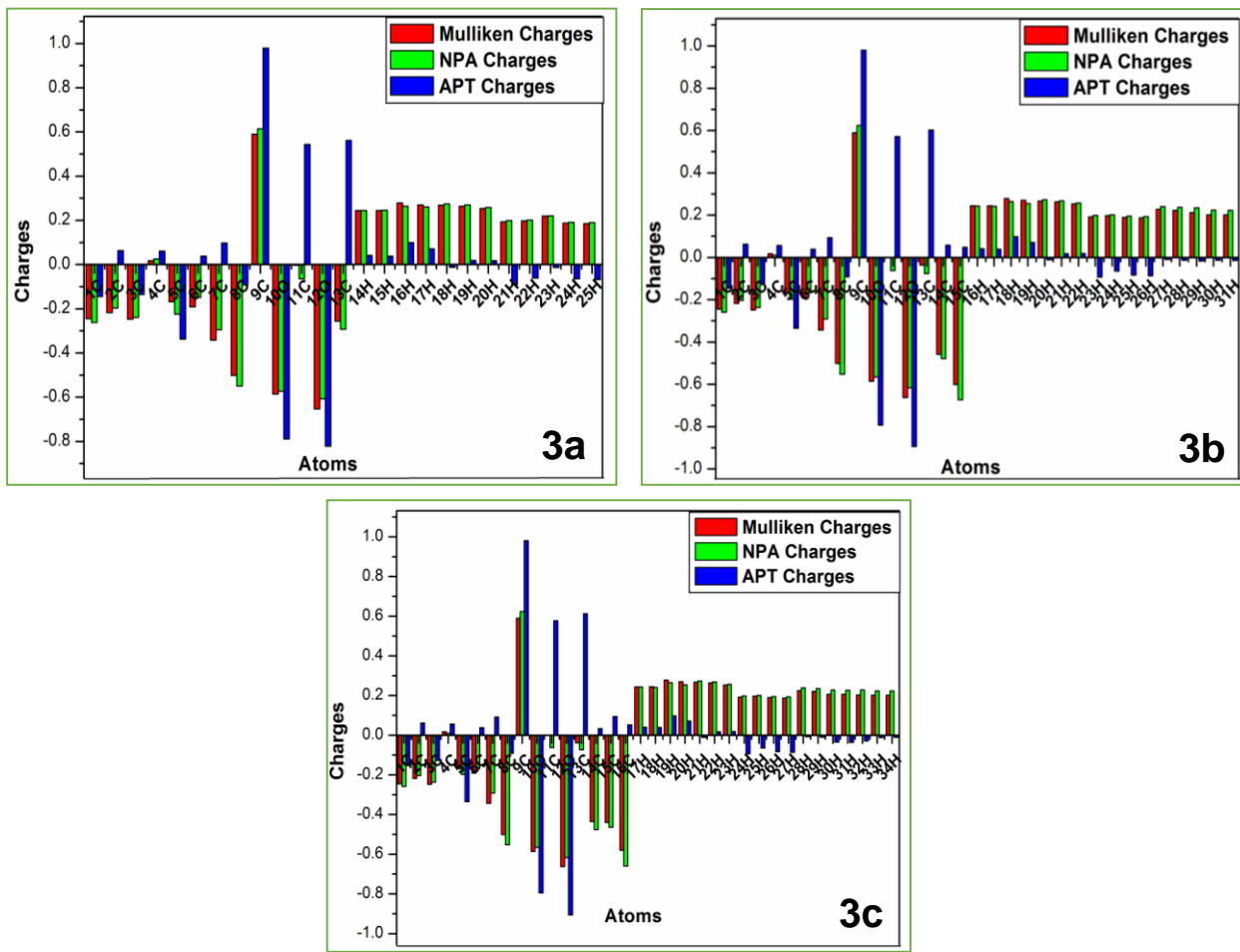


Figure S3. The Mulliken atomic charges of compounds, 3a, 3b, and 3c.

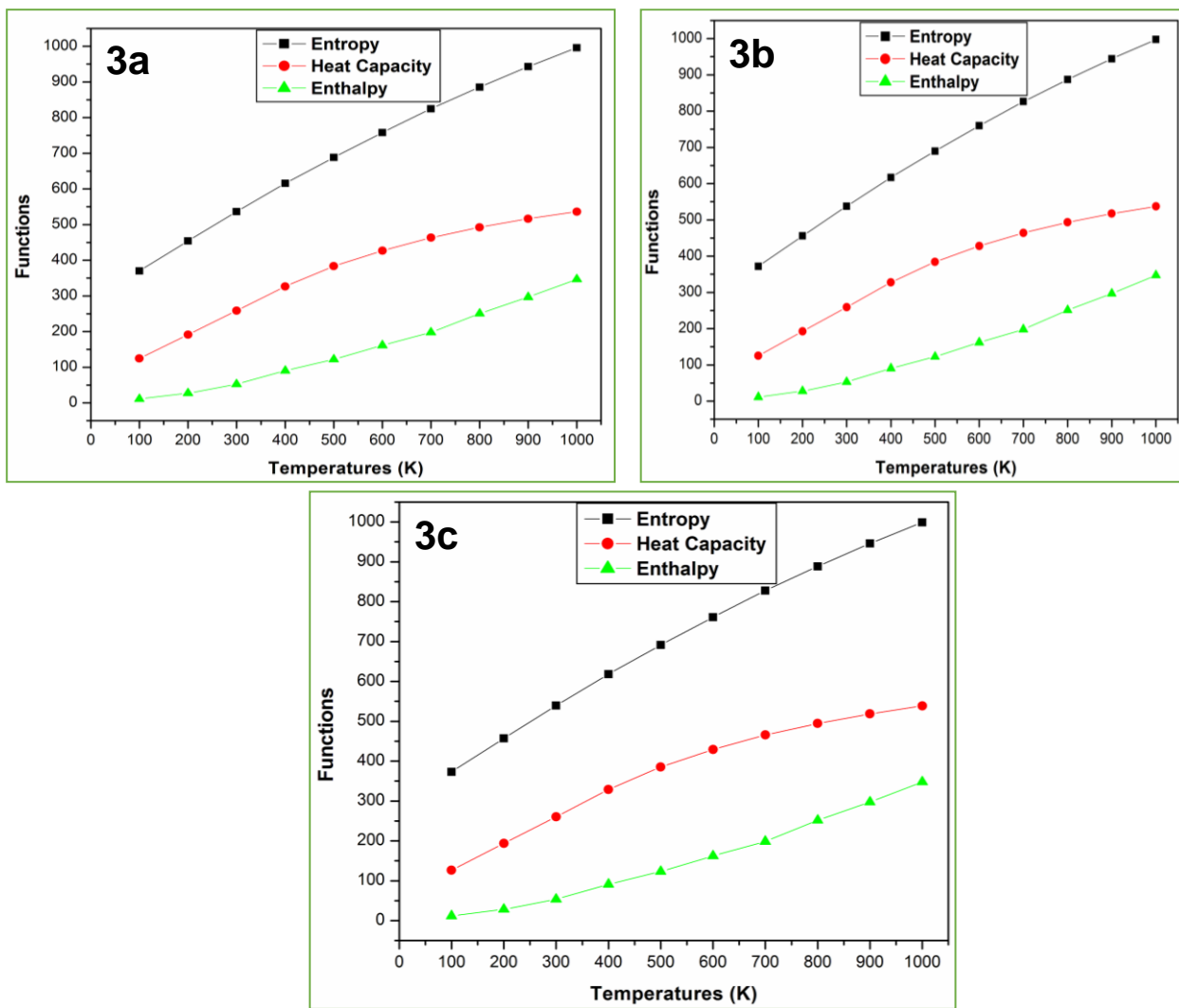


Figure S4. The thermodynamic properties at different temperatures of compounds 3a, 3b, and 3c.

Table S1. The PES scans and the total energy values of 3a, 3b, and 3c compounds.

Compounds		3a	3b	3c
Scan Step Number	Scan Steps at Degree	Total Energy (Hartree)	Total Energy (Hartree)	Total Energy (Hartree)
1	10	-570.061	-647.705	-686.524
2	20	-570.061	-647.706	-686.525
3	30	-570.063	-647.707	-686.526
4	40	-570.066	-647.710	-686.529
5	50	-570.068	-647.712	-686.531
6	60	-570.070	-647.714	-686.533
7	70	-570.071	-647.715	-686.534
8	80	-570.071	-647.715	-686.535
9	90	-570.070	-647.715	-686.534
10	100	-570.068	-647.713	-686.532
11	110	-570.066	-647.710	-686.529
12	120	-570.065	-647.709	-686.528
13	130	-570.064	-647.709	-686.528
14	140	-570.065	-647.710	-686.529
15	150	-570.067	-647.712	-686.531
16	160	-570.070	-647.714	-686.533
17	170	-570.072	-647.716	-686.535
18	180	-570.073	-647.717	-686.536
19	190	-570.074	-647.718	-686.537
20	200	-570.073	-647.717	-686.536
21	210	-570.071	-647.715	-686.534
22	220	-570.069	-647.713	-686.532
23	230	-570.067	-647.711	-686.530
24	240	-570.065	-647.709	-686.528
25	250	-570.064	-647.708	-686.527
26	260	-570.066	-647.710	-686.529

27	270	-570.068	-647.712	-686.531
28	280	-570.071	-647.715	-686.534
29	290	-570.073	-647.718	-686.537
30	300	-570.075	-647.719	-686.538
31	310	-570.074	-647.719	-686.538
32	320	-570.073	-647.717	-686.536
33	330	-570.071	-647.715	-686.534
34	340	-570.068	-647.712	-686.531
35	350	-570.064	-647.708	-686.527
36	360	-570.062	-647.702	-686.525

Table S2. The optimized bond parameters of 3a, 3b, and 3c compounds.

3a			
Bond Lengths (Å)	B3LYP/ 6-311++G(d,p)	Bond Lengths (Å)	B3LYP/ 6-311++G(d,p)
R(1,2)	1.3926	R(7,11)	1.5254
R(1,6)	1.3801	R(7,18)	1.0821
R(1,14)	1.0716	R(8,9)	1.5325
R(2,3)	1.3842	R(8,19)	1.0821
R(2,15)	1.0725	R(8,20)	1.0851
R(3,4)	1.3838	R(9,10)	1.2099
R(3,16)	1.0679	R(11,12)	1.4358
R(4,5)	1.3791	R(11,21)	1.0865
R(4,7)	1.5234	R(11,22)	1.0855
R(5,6)	1.382	R(12,13)	1.4355
R(5,9)	1.4742	R(13,23)	1.079
R(6,17)	1.0719	R(13,24)	1.085
R(7,8)	1.5531	R(13,25)	1.0852
Bond Angles (°)	B3LYP/ 6-311++G(d,p)	Bond Angles (°)	B3LYP/ 6-311++G(d,p)
A(2,1,6)	119.9385	A(11,7,18)	107.7542
A(2,1,14)	119.7669	A(7,8,9)	106.4416
A(6,1,14)	120.2946	A(7,8,19)	112.5906
A(1,2,3)	121.3609	A(7,8,20)	111.8645
A(1,2,15)	119.2684	A(9,8,19)	109.6418
A(3,2,15)	119.3707	A(9,8,20)	108.3167
A(2,3,4)	118.4279	A(19,8,20)	107.8994
A(2,3,16)	121.6595	A(5,9,8)	106.8861
A(4,3,16)	119.9018	A(5,9,10)	126.8695
A(3,4,5)	119.958	A(8,9,10)	126.2424
A(3,4,7)	128.3747	A(7,11,12)	107.0351
A(5,4,7)	111.6629	A(7,11,21)	110.3055
A(4,5,6)	121.9577	A(7,11,22)	110.0859
A(4,5,9)	111.0518	A(12,11,21)	110.0218
A(6,5,9)	126.9902	A(12,11,22)	110.7938
A(1,6,5)	118.3566	A(21,11,22)	108.5987
A(1,6,17)	121.7188	A(11,12,13)	114.872

A(5,6,17)	119.9247	A(12,13,23)	106.8307
A(4,7,8)	103.8276	A(12,13,24)	111.2652
A(4,7,11)	111.9158	A(12,13,25)	111.2014
A(4,7,18)	109.907	A(23,13,24)	109.3977
A(8,7,11)	112.0764	A(23,13,25)	109.2964
A(8,7,18)	111.3761	A(24,13,25)	108.8079
Dihedral Angles (°)	B3LYP/ 6-311++G(d,p)	Dihedral Angles (°)	B3LYP/ 6-311++G(d,p)
D(6,1,2,3)	0.1506	D(6,5,9,8)	-178.4955
D(6,1,2,15)	-179.7984	D(6,5,9,10)	1.0074
D(14,1,2,3)	-179.9156	D(4,7,8,9)	3.5742
D(14,1,2,15)	0.1354	D(4,7,8,19)	123.7317
D(2,1,6,5)	-0.1638	D(4,7,8,20)	-114.5564
D(2,1,6,17)	179.838	D(11,7,8,9)	124.5463
D(14,1,6,5)	179.9028	D(11,7,8,19)	-115.2961
D(14,1,6,17)	-0.0954	D(11,7,8,20)	6.4158
D(1,2,3,4)	0.0471	D(18,7,8,9)	-114.6487
D(1,2,3,16)	-178.7548	D(18,7,8,19)	5.5088
D(15,2,3,4)	179.996	D(18,7,8,20)	127.2208
D(15,2,3,16)	1.1941	D(4,7,11,12)	-67.6081
D(2,3,4,5)	-0.2265	D(4,7,11,21)	172.7096
D(2,3,4,7)	178.9431	D(4,7,11,22)	52.8816
D(16,3,4,5)	178.5971	D(8,7,11,12)	176.2133
D(16,3,4,7)	-2.2333	D(8,7,11,21)	56.5309
D(3,4,5,6)	0.2163	D(8,7,11,22)	-63.2971
D(3,4,5,9)	-179.5953	D(18,7,11,12)	53.3351
D(7,4,5,6)	-179.0832	D(18,7,11,21)	-66.3473
D(7,4,5,9)	1.1052	D(18,7,11,22)	173.8247
D(3,4,7,8)	177.8063	D(7,8,9,5)	-3.0833
D(3,4,7,11)	56.7263	D(7,8,9,10)	177.4097
D(3,4,7,18)	-62.9612	D(19,8,9,5)	-125.1288
D(5,4,7,8)	-2.9678	D(19,8,9,10)	55.3643
D(5,4,7,11)	-124.0479	D(20,8,9,5)	117.3612
D(5,4,7,18)	116.2646	D(20,8,9,10)	-62.1457
D(4,5,6,1)	-0.0171	D(7,11,12,13)	178.0738
D(4,5,6,17)	179.9811	D(21,11,12,13)	-62.0618
D(9,5,6,1)	179.7628	D(22,11,12,13)	58.0363

D(9,5,6,17)	-0.2389	D(11,12,13,23)	179.6781
D(4,5,9,8)	1.3044	D(11,12,13,24)	-60.9768
D(4,5,9,10)	-179.1926	D(11,12,13,25)	60.4919

3b

Bond Lengths (Å)	B3LYP/ 6-311++G(d,p)	Bond Lengths (Å)	B3LYP/ 6-311++G(d,p)
R(1,2)	1.3926	R(8,21)	1.0821
R(1,6)	1.3801	R(8,22)	1.0851
R(1,16)	1.0716	R(9,10)	1.2099
R(2,3)	1.3841	R(11,12)	1.4355
R(2,17)	1.0725	R(11,23)	1.0864
R(3,4)	1.3838	R(11,24)	1.0854
R(3,18)	1.0678	R(12,13)	1.439
R(4,5)	1.3791	R(13,14)	1.5258
R(4,7)	1.5234	R(13,25)	1.086
R(5,6)	1.382	R(13,26)	1.0864
R(5,9)	1.4742	R(14,15)	1.5392
R(6,19)	1.0719	R(14,27)	1.0829
R(7,8)	1.5532	R(14,28)	1.0832
Bond Angles (°)	B3LYP/ 6-311++G(d,p)	Bond Angles (°)	B3LYP/ 6-311++G(d,p)
A(2,1,6)	119.9344	A(21,8,22)	107.8949
A(2,1,16)	119.7697	A(5,9,8)	106.8839
A(6,1,16)	120.2958	A(5,9,10)	126.8601
A(1,2,3)	121.3565	A(8,9,10)	126.2542
A(1,2,17)	119.2653	A(7,11,12)	107.1333
A(3,2,17)	119.3782	A(7,11,23)	110.2087
A(2,3,4)	118.4414	A(7,11,24)	110.0653
A(2,3,18)	121.6651	A(12,11,23)	110.0276
A(4,3,18)	119.8829	A(12,11,24)	110.8144
A(3,4,5)	119.9455	A(23,11,24)	108.591
A(3,4,7)	128.3758	A(11,12,13)	115.576
A(5,4,7)	111.6741	A(12,13,14)	107.3969
A(4,5,6)	121.9623	A(12,13,25)	110.218
A(4,5,9)	111.0492	A(12,13,26)	110.065
A(6,5,9)	126.9883	A(14,13,25)	110.56
A(1,6,5)	118.3593	A(14,13,26)	110.4029

A(1,6,19)	121.7165	A(25,13,26)	108.2057
A(5,6,19)	119.9242	A(13,14,15)	111.4929
A(4,7,8)	103.818	A(13,14,27)	108.2588
A(4,7,11)	111.9597	A(13,14,28)	108.3819
A(4,7,20)	109.9042	A(15,14,27)	110.5315
A(8,7,11)	112.0488	A(15,14,28)	110.3677
A(8,7,20)	111.3719	A(27,14,28)	107.6896
A(11,7,20)	107.755	A(14,15,29)	110.781
Dihedral Angles (°)	B3LYP/ 6-311++G(d,p)	Dihedral Angles (°)	B3LYP/ 6-311++G(d,p)
D(6,1,2,3)	0.1393	D(20,7,8,21)	5.3999
D(6,1,2,17)	-179.8108	D(20,7,8,22)	127.101
D(16,1,2,3)	-179.9223	D(4,7,11,12)	-67.646
D(16,1,2,17)	0.1276	D(4,7,11,23)	172.6604
D(2,1,6,5)	-0.1636	D(4,7,11,24)	52.9162
D(2,1,6,19)	179.8487	D(8,7,11,12)	176.1768
D(16,1,6,5)	179.8983	D(8,7,11,23)	56.4832
D(16,1,6,19)	-0.0894	D(8,7,11,24)	-63.261
D(1,2,3,4)	0.0526	D(20,7,11,12)	53.3212
D(1,2,3,18)	-178.7608	D(20,7,11,23)	-66.3724
D(17,2,3,4)	-179.9974	D(20,7,11,24)	173.8833
D(17,2,3,18)	1.1892	D(7,8,9,5)	-2.9843
D(2,3,4,5)	-0.2152	D(7,8,9,10)	177.4849
D(2,3,4,7)	178.9307	D(21,8,9,5)	-125.0238
D(18,3,4,5)	178.62	D(21,8,9,10)	55.4454
D(18,3,4,7)	-2.2341	D(22,8,9,5)	117.4711
D(3,4,5,6)	0.1933	D(22,8,9,10)	-62.0596
D(3,4,5,9)	-179.6418	D(7,11,12,13)	178.9165
D(7,4,5,6)	-179.0862	D(23,11,12,13)	-61.2739
D(7,4,5,9)	1.0787	D(24,11,12,13)	58.8316
D(3,4,7,8)	177.9157	D(11,12,13,14)	179.3581
D(3,4,7,11)	56.8516	D(11,12,13,25)	-60.1391
D(3,4,7,20)	-62.8633	D(11,12,13,26)	59.1342
D(5,4,7,8)	-2.8807	D(12,13,14,15)	-179.1818
D(5,4,7,11)	-123.9448	D(12,13,14,27)	-57.3903
D(5,4,7,20)	116.3402	D(12,13,14,28)	59.1489
D(4,5,6,1)	-0.0001	D(25,13,14,15)	60.5322

D(4,5,6,19)	179.9878	D(25,13,14,27)	-177.6763
D(9,5,6,1)	179.8072	D(25,13,14,28)	-61.1371
D(9,5,6,19)	-0.2049	D(26,13,14,15)	-59.1726
D(4,5,9,8)	1.2571	D(26,13,14,27)	62.6189
D(4,5,9,10)	-179.2159	D(26,13,14,28)	179.1581

3c

Bond Lengths (Å)	B3LYP/ 6-311++G(d,p)	Bond Lengths (Å)	B3LYP/ 6-311++G(d,p)
R(1,2)	1.3926	R(9,10)	1.2099
R(1,6)	1.3801	R(11,12)	1.4355
R(1,17)	1.0716	R(11,24)	1.0864
R(2,3)	1.3841	R(11,25)	1.0854
R(2,18)	1.0725	R(12,13)	1.4394
R(3,4)	1.3838	R(13,14)	1.5259
R(3,19)	1.0678	R(13,26)	1.086
R(4,5)	1.3791	R(13,27)	1.0863
R(4,7)	1.5234	R(14,15)	1.5389
R(5,6)	1.382	R(14,28)	1.0837
R(5,9)	1.4742	R(14,29)	1.084
R(6,20)	1.0719	R(15,16)	1.5407
R(7,8)	1.5532	R(15,30)	1.0859
R(7,11)	1.5261	R(15,31)	1.0859
R(7,21)	1.0821	R(16,32)	1.0841
Bond Angles (°)	B3LYP/ 6-311++G(d,p)	Bond Angles (°)	B3LYP/ 6-311++G(d,p)
A(2,1,6)	119.9342	A(8,9,10)	126.2551
A(2,1,17)	119.7699	A(7,11,12)	107.124
A(6,1,17)	120.2959	A(7,11,24)	110.2081
A(1,2,3)	121.3579	A(7,11,25)	110.0652
A(1,2,18)	119.2644	A(12,11,24)	110.0344
A(3,2,18)	119.3777	A(12,11,25)	110.8194
A(2,3,4)	118.4398	A(24,11,25)	108.5893
A(2,3,19)	121.6693	A(11,12,13)	115.5682
A(4,3,19)	119.8802	A(12,13,14)	107.377
A(3,4,5)	119.9461	A(12,13,26)	110.1655
A(3,4,7)	128.3755	A(12,13,27)	110.0115
A(5,4,7)	111.6737	A(14,13,26)	110.6229

A(4,5,6)	121.9625	A(14,13,27)	110.4696
A(4,5,9)	111.0489	A(26,13,27)	108.2015
A(6,5,9)	126.9883	A(13,14,15)	112.0399
A(1,6,5)	118.359	A(13,14,28)	108.3094
A(1,6,20)	121.7168	A(13,14,29)	108.4363
A(5,6,20)	119.9242	A(15,14,28)	110.2038
A(4,7,8)	103.8171	A(15,14,29)	110.0428
A(4,7,11)	111.9624	A(28,14,29)	107.6834
A(4,7,21)	109.8994	A(14,15,16)	111.8524
A(8,7,11)	112.0568	A(14,15,30)	109.4765
A(8,7,21)	111.37	A(14,15,31)	109.4492
A(11,7,21)	107.7518	A(16,15,30)	109.3425
Dihedral Angles (°)	B3LYP/ 6-311++G(d,p)	Dihedral Angles (°)	B3LYP/ 6-311++G(d,p)
D(6,1,2,3)	0.1405	D(8,7,11,12)	176.1809
D(6,1,2,18)	-179.81	D(8,7,11,24)	56.4851
D(17,1,2,3)	-179.9219	D(8,7,11,25)	-63.2566
D(17,1,2,18)	0.1276	D(21,7,11,12)	53.3247
D(2,1,6,5)	-0.1642	D(21,7,11,24)	-66.3711
D(2,1,6,20)	179.8471	D(21,7,11,25)	173.8872
D(17,1,6,5)	179.8986	D(7,8,9,5)	-3.0175
D(17,1,6,20)	-0.0901	D(7,8,9,10)	177.4558
D(1,2,3,4)	0.053	D(22,8,9,5)	-125.0643
D(1,2,3,19)	-178.7586	D(22,8,9,10)	55.4091
D(18,2,3,4)	-179.9965	D(23,8,9,5)	117.4296
D(18,2,3,19)	1.1919	D(23,8,9,10)	-62.0971
D(2,3,4,5)	-0.2178	D(7,11,12,13)	178.9193
D(2,3,4,7)	178.9237	D(24,11,12,13)	-61.2736
D(19,3,4,5)	178.6156	D(25,11,12,13)	58.8374
D(19,3,4,7)	-2.2429	D(11,12,13,14)	179.4015
D(3,4,5,6)	0.1967	D(11,12,13,26)	-60.0621
D(3,4,5,9)	-179.6364	D(11,12,13,27)	59.1398
D(7,4,5,6)	-179.0791	D(12,13,14,15)	-179.1176
D(7,4,5,9)	1.0878	D(12,13,14,28)	-57.3539
D(3,4,7,8)	177.8905	D(12,13,14,29)	59.2343
D(3,4,7,11)	56.8159	D(26,13,14,15)	60.6359
D(3,4,7,21)	-62.8935	D(26,13,14,28)	-177.6004

D(5,4,7,8)	-2.9099	D(26,13,14,29)	-61.0122
D(5,4,7,11)	-123.9846	D(27,13,14,15)	-59.1471
D(5,4,7,21)	116.306	D(27,13,14,28)	62.6167
D(4,5,6,1)	-0.0018	D(27,13,14,29)	179.2048
D(4,5,6,20)	179.987	D(13,14,15,16)	-179.8885
D(9,5,6,1)	179.8032	D(13,14,15,30)	-58.5332
D(4,5,9,8)	1.2728	D(28,14,15,16)	59.4399

Table S3. The NBO analysis of 3a, 3b, and 3c compounds.

3a							
Type	Donor NBO (i)	ED/e	Acceptor NBO (j)	ED/e	E ⁽²⁾ KJ/mol	E(j)-E(i) a.u.	F(i, j) a.u.
$\pi -\pi^*$	BD (2) C1-C6	1.66285	BD*(2) C2-C3	0.3002	198.95	0.51	0.141
			BD*(2) C4-C5	0.37963	165.23	0.51	0.129
$\pi -\pi^*$	BD (2) C2-C3	1.6514	BD*(2) C1-C6	0.28405	154.68	0.51	0.125
			BD*(2) C4-C5	0.37963	217.69	0.51	0.147
$\pi -\pi^*$	BD (2) C4-C5	1.63796	BD*(2) C1-C6	0.28405	183.13	0.52	0.137
			BD*(2) C9-O10	0.13112	184.51	0.53	0.145
$\pi -\pi^*$	BD (2) C9-O10	1.97729	BD*(2) C4-C5	0.37963	34.69	0.69	0.074
			BD*(1) C8-H19	0.00674	5.06	1.14	0.033
n - σ^*	LP (2) O10	1.91095	BD*(1) C5-C9	0.05336	90.12	1.34	0.153
			BD*(1) C8-C9	0.055	130.71	1.04	0.162
n - σ^*	LP (2) O12	1.9384	BD*(1) C11-H21	0.02293	37.2	1.1	0.089
			BD*(1) C11-H22	0.02376	35.19	1.1	0.087
			BD*(1) C13-H25	0.0188	36.82	1.1	0.089
$\pi^*-\sigma^*$	BD*(2) C4-C5	0.37963	BD*(1) C7-C11	0.02076	9.2	0.4	0.059
			BD*(2) C9-O10	0.13112	1246.92	0.01	0.115
3b							
Type	Donor NBO (i)	ED/e	Acceptor NBO (j)	ED/e	E ⁽²⁾ KJ/mol	E(j)-E(i) a.u.	F(i, j) a.u.
$\pi -\pi^*$	BD (2) C1-C6	1.66302	BD*(2) C2-C3	0.30026	198.95	0.51	0.141
			BD*(2) C4-C5	0.37925	165.1	0.51	0.129
$\pi -\pi^*$	BD (2) C2-C3	1.65174	BD*(2) C1-C6	0.28409	154.68	0.51	0.125
			BD*(2) C4-C5	0.37925	217.44	0.51	0.147
$\pi -\pi^*$	BD (2) C4-C5	1.63789	BD*(2) C1-C6	0.28409	183.3	0.52	0.137
			BD*(2) C2-C3	0.30026	143.18	0.52	0.121
			BD*(2) C9-O10	0.13105	184.47	0.53	0.145
$\pi -\pi^*$	BD (2) C9-O10	1.97729	BD*(2) C4-C5	0.37925	34.64	0.69	0.074
			BD*(1) C8-H21	0.00674	5.1	1.14	0.033
			BD*(1) C8-H22	0.00791	4.52	1.13	0.031
n - σ^*	LP (2) O10	1.91097	BD*(1) C5-C9	0.05337	90.12	1.34	0.153
			BD*(1) C8-C9	0.05498	130.67	1.04	0.162
n - σ^*	LP (2) O12	1.93806	BD*(1) C11-H23	0.02287	37.45	1.1	0.09
			BD*(1) C13-H26	0.02421	38.37	1.1	0.091
$\pi^*-\sigma^*$	BD*(2) C4-C5	0.37925	BD*(1) C7-C11	0.02055	9.16	0.4	0.059

			BD*(2) C9-O10	0.13105	1253.48	0.01	0.115
3c							
Type	Donor NBO (i)	ED/e	Acceptor NBO (j)	ED/e	E ⁽²⁾ KJ/mol	E(j)-E(i) a.u.	F(i, j) a.u.
π -π*	BD (2) C1-C6	1.67212	BD*(2) C2-C3	0.29872	184.22	0.49	0.132
			BD*(2) C4-C5	0.36393	157.49	0.49	0.122
π -π*	BD (2) C2-C3	1.66178	BD*(2) C1-C6	0.28951	148.41	0.49	0.119
			BD*(2) C4-C5	0.36393	204.11	0.49	0.138
π -π*	BD (2) C4-C5	1.651	BD*(2) C1-C6	0.28951	177.28	0.49	0.131
			BD*(2) C2-C3	0.29872	139.87	0.49	0.116
			BD*(2) C9-O10	0.10404	127.57	0.52	0.119
π -π*	BD (2) C9-O10	1.98365	BD*(2) C4-C5	0.36393	22.55	0.68	0.059
			BD*(1) C8-H23	0.00757	5.06	1.19	0.034
n -σ*	LP (2) O10	1.90216	BD*(1) C5-C9	0.05861	113.3	1.14	0.158
			BD*(1) C8-C9	0.05366	128.53	1.02	0.16
n -σ*	LP (2) O12	1.9454	BD*(1) C11-H24	0.01981	35.1	1.16	0.089
			BD*(1) C13-H27	0.02074	33.56	1.16	0.087
π*-σ*	BD*(2) C4-C5	0.36393	BD*(1) C7-C11	0.01923	6.36	0.42	0.052
			BD*(2) C9-O10	0.10404	442.71	0.02	0.094

Table S4. The Mulliken, NPA, and APT charges of 3a, 3b, and 3c compounds.

3a			
Atoms	Mulliken Charges	NPA Charges	APT Charges
1C	-0.24505	-0.26224	-0.144282
2C	-0.217886	-0.19708	0.06337
3C	-0.246705	-0.23972	-0.135799
4C	0.017115	0.02518	0.060566
5C	-0.168757	-0.22414	-0.337579
6C	-0.191667	-0.14952	0.038173
7C	-0.341738	-0.29524	0.097425
8C	-0.501631	-0.54986	-0.092016
9C	0.590127	0.61361	0.979102
10O	-0.58558	-0.57352	-0.789142
11C	-0.003099	-0.06503	0.543457
12O	-0.653737	-0.60775	-0.822143
13C	-0.256353	-0.29261	0.56134
14H	0.244043	0.24443	0.041391
15H	0.244949	0.24547	0.038189
16H	0.278795	0.26393	0.099447
17H	0.270034	0.25992	0.071386
18H	0.268225	0.2738	-0.011811
19H	0.263699	0.27014	0.01898
20H	0.253148	0.25792	0.017771
21H	0.192822	0.19879	-0.09004
22H	0.197583	0.20164	-0.061028
23H	0.219555	0.22104	-0.013751
24H	0.18745	0.19119	-0.06476
25H	0.184657	0.18964	-0.068246
3b			
Atoms	Mulliken Charges	NPA Charges	APT Charges
1C	-0.244966	-0.25881	-0.145164
2C	-0.218036	-0.20317	0.062053
3C	-0.248023	-0.23692	-0.129141
4C	0.017498	0.01044	0.056659
5C	-0.16873	-0.19743	-0.33513
6C	-0.191662	-0.16789	0.038452

7C	-0.343043	-0.29169	0.093233
8C	-0.501534	-0.55261	-0.091751
9C	0.5901	0.62348	0.97999
10O	-0.585711	-0.56517	-0.793546
11C	-0.00169	-0.06237	0.571212
12O	-0.66232	-0.61696	-0.894155
13C	-0.035454	-0.07582	0.602718
14C	-0.458621	-0.47912	0.05818
15C	-0.600742	-0.67381	0.048328
16H	0.243958	0.24314	0.04074
17H	0.244592	0.24144	0.038851
18H	0.278435	0.26435	0.097584
19H	0.270017	0.25472	0.071007
20H	0.267182	0.27275	-0.011353
21H	0.263468	0.26815	0.017794
22H	0.253287	0.25714	0.019008
23H	0.192135	0.19862	-0.092999
24H	0.197375	0.20106	-0.064211
25H	0.189937	0.19493	-0.083451
26H	0.186953	0.19303	-0.086823
27H	0.227274	0.24061	-0.010359
28H	0.22323	0.23704	-0.01317
29H	0.21264	0.2342	-0.017208
30H	0.201372	0.22343	-0.013144
31H	0.201081	0.22326	-0.014205

3c

Atoms	Mulliken Charges	NPA Charges	APT Charges
1C	-0.244977	-0.25883	-0.145376
2C	-0.218059	-0.20321	0.061477
3C	-0.248094	-0.23691	-0.127416
4C	0.017492	0.01048	0.055854
5C	-0.168746	-0.19745	-0.334751
6C	-0.191684	-0.16792	0.038464
7C	-0.343066	-0.29168	0.091919
8C	-0.501519	-0.55261	-0.091433
9C	0.590079	0.6235	0.980723
10O	-0.585765	-0.56523	-0.795082

11C	-0.00176	-0.06238	0.577443
12O	-0.662406	-0.61656	-0.906109
13C	-0.03848	-0.07344	0.612439
14C	-0.434929	-0.47576	0.032718
15C	-0.440358	-0.46425	0.094232
16C	-0.579454	-0.6602	0.051877
17H	0.243897	0.24311	0.04058
18H	0.244501	0.24139	0.039003
19H	0.278677	0.26448	0.097133
20H	0.269972	0.25469	0.070855
21H	0.267166	0.27275	-0.011078
22H	0.263401	0.26811	0.017501
23H	0.25328	0.25713	0.019296
24H	0.192019	0.19855	-0.093896
25H	0.197252	0.20099	-0.06512
26H	0.190115	0.19502	-0.082671
27H	0.187137	0.19313	-0.085963
28H	0.224365	0.23861	-0.007948
29H	0.220246	0.23496	-0.010447
30H	0.20691	0.22741	-0.035115
31H	0.206618	0.22724	-0.036041
32H	0.203266	0.22807	-0.029365
33H	0.201742	0.22358	-0.012286
34H	0.201164	0.22323	-0.011415

Table S5. The Thermodynamic properties at different temperatures of 3a, 3b, and 3c compounds.

3a			
T	S(J/mol.K)	Cp(J/mol.K)	ddH(kJ/mol)
100	370.21	124.43	10.87
200	454.17	191.58	27.22
300	536.29	258.41	52.47
400	615.32	326.51	90.12
500	688.21	383.24	122.18
600	758.02	426.81	161.37
700	824.71	463.23	197.68
800	885.51	492.24	250.68
900	942.72	516.31	296.45
1000	995.91	536.19	346.72
3b			
T	S(J/mol.K)	Cp(J/mol.K)	ddH(kJ/mol)
100	371.71	125.43	11.37
200	455.67	192.58	27.72
300	537.79	259.41	52.97
400	616.82	327.51	90.62
500	689.71	384.24	122.68
600	759.52	427.81	161.87
700	826.21	464.23	198.18
800	887.01	493.24	251.18
900	944.22	517.31	296.95
1000	997.41	537.19	347.22
3c			
T	S(J/mol.K)	Cp(J/mol.K)	ddH(kJ/mol)
100	373.16	126.68	11.93
200	457.12	193.83	28.28
300	539.24	260.66	53.53
400	618.27	328.76	91.18
500	691.16	385.49	123.24
600	760.97	429.06	162.43
700	827.66	465.48	198.74
800	888.46	494.49	251.74
900	945.67	518.56	297.51

1000	998.86	538.44	347.78
------	--------	--------	--------

Anti-inflammatory activity by BSA denaturation technique

The synthesized compound and standard diclofenac sodium were screened for anti-inflammatory activity by using the inhibition of albumin denaturation technique with minor modification. The standard drug and compound were dissolved in a minimum quantity of Dimethyl formamide (DMF) and diluted with phosphate buffer (0.2 M, pH 7.4). The final concentration of DMF in all solutions was less than 2.5%. Test Solution (2.5 mL) containing different concentrations of the drug was mixed with 1 mL of 1 mM Bovine serum albumin solution in phosphate buffer and incubated at 37 °C in an incubator for 10 min. Denaturation was induced by keeping the reaction mixture at 70 °C in a water bath for 10 min. After cooling, the turbidity was measured at 660 nm. Percentage of Inhibition of denaturation was calculated from control where no drug was added. The percentage inhibition of denaturation was calculated by using the following formula.

$$\% \text{ of Inhibition} = 100 \times [A_c - A_t / A_c]$$

A_t: Absorbance of test

A_c: Absorbance of control

Anti-diabetic activity α -amylase inhibition technique

The antidiabetic activity of the samples was performed using the α -amylase inhibition method. Briefly, Amylase (0.2%) was incubated with and without samples (in 1.5 mL) and standard for 10 min at 25 °C. This experiment was performed in 0.2 M phosphate buffer (pH 6.9). After pre-incubation, the 1% starch solution (0.5 mL) was added and the reaction mixture was incubated for 30 min at 25 °C. To stop the enzymatic reaction, DNSA reagent (0.5 mL) was added as the color reagent and then incubated in a boiling water bath for 90 min. After cooling down to room temperature, 0.5 mL of samples were diluted to 2.5 mL of distilled water and the absorbance was measured at 540 nm using a UV-visible spectrophotometer. The measured absorbance was compared with that of the control experiment. The percentage inhibition was calculated from the given formula.

$$\% \text{ of Inhibition} = 100 \times [A_c - A_t / A_c]$$

A_t : Absorbance of test

A_c : Absorbance of control

Table S6. Anti-inflammation activity of synthesized compounds.

Concentration ($\mu\text{g/ml}$)	Inhibition (%)			
	3a	3b	3c	std
20	28.31	29.92	31.29	21.32
40	36.41	37.41	42.02	31.05
80	49.75	50.50	55.36	44.39
200	63.47	64.34	68.46	57.85
400	80.92	83.17	88.41	76.56

Table S7. Anti-diabetic activity of synthesized compounds.

Concentration ($\mu\text{g/ml}$)	Inhibition (%)			
	3a	3b	3c	std
20	28.47	31.45	32.41	27.45
40	46.41	47.92	49.96	42.66
80	60.59	61.21	64.31	58.52
200	83.21	84.27	86.90	81.55
400	89.42	90.14	92.54	85.12

References

- S1. Frisch, M.J., Trucks, G.W., Schlegel, H.B., Scuseria, G.E., Robb, M.A., Cheeseman, J.R., Scalmani, G., Barone, V., Mennucci, B., Petersson, G.A., Nakatsuji, H., Caricato, M., Li, X., Hratchian, H.P., Izmaylov, A.F., Bloino, J., Zheng, G., Sonnenberg, J.L., Hada, M., Ehara, M., Toyota, K., Fukuda, R., Hasegawa, J., Ishida, M., Nakajima, T., Honda, Y., Kitao, O., Nakai,

H., Vreven, T., Montgomery Jr., J.A., Peralta, J.E., Ogliaro, F., Bearpark, M., Heyd, J.J., Brothers, E., Kudin, K.N., Staroverov, V.N., Keith, T., Kobayashi, R., Normand, J., Raghavachari, K., Rendell, A., Burant, J.C., Iyengar, S.S., Tomasi, J., Cossi, M., Rega, N., Millam, J.M., Klene, M., Knox, J.E., Cross, J.B., Bakken, V., Adamo, C., Jaramillo, J., Gomperts, R., Stratmann, R.E., Yazyev, O., Austin, A.J., Cammi, R., Pomelli, C., Ochterski, J.W., Martin, R.L., Morokuma, K., Zakrzewski, V.G., Voth, G.A., Salvador, P., Dannenberg, J.J., Dapprich, S., Daniels, A.D., Farkas, O., Foresman, J.B., Ortiz, J.V., Cioslowski, J., Fox, D.J. Gaussian 09, Revision C.02, Gaussian Inc., Wallingford CT, **(2010)**.

S2. Bikadi, Z. and Hazai, E., Application of the PM6 semi-empirical method to modeling proteins enhances docking accuracy of AutoDock. *Journal of cheminformatics*, 1, **(2009)**, pp.1-16.

S3. Morris, G.M., Goodsell, D.S., Halliday, R.S., Huey, R., Hart, W.E., Belew, R.K. and Olson, A.J., Automated docking using a Lamarckian genetic algorithm and an empirical binding free energy function. *Journal of computational chemistry*, 19(14), **(1998)**, pp.1639-1662.